AD-A250 305

Total-Dose-Induced Charge Buildup
in Nitrided-Oxide MOS Devices

Prepared by

R. J. KRANTZ and J. SCARPULLA
Electronics Technology Center
Technology Operations
The Aerospace Corporation

and

J. CABLE
TRW Corporation
One Space Park
Redondo Beach, CA 90278

23 April 1992

Prepared for

Engineering and Technology Group

THE AEROSPACE CORPORATION
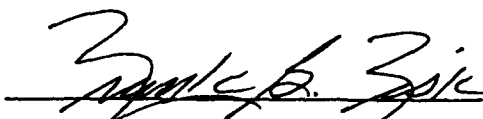El Segundo, California

92-12930

92 5 14 050

This report was submitted by The Aerospace Corporation, El Segundo, CA 90245-4691, under Contract No. F04701-88-C-0089 with the Space Systems Division, P. O. Box 92960, Los Angeles, CA 90009-2960. It was reviewed and approved for The Aerospace Corporation by B. K. Janousek, Principal Director, Electronics Technology Center. Capt. Martin Williams was the project officer for the Mission-Oriented Investigation and Experimentation (MOIE) program.

This report has been reviewed by the Public Affairs Office (PAS) and is releasable to the National Technical Information Service (NTIS). At NTIS, it will be available to the general public, including foreign nationals.

This technical report has been reviewed and is approved for publication. Publication of this report does not constitute Air Force approval of the report's findings or conclusions. It is published only for the exchange and stimulation of ideas.

MARTIN K. WILLIAMS, Capt, USAF
MOIE Projects Manager

FRANKLIN B. FISK, GM-14, DAF
Deputy Chief, Space Sensors Division

REPORT DOCUMENTATION PAGE

1a. REPORT SECURITY CLASSIFICATION	1b. RESTRICTIVE MARKINGS
Unclassified	

2a. SECURITY CLASSIFICATION AUTHORITY	3. DISTRIBUTION/AVAILABILITY OF REPORT
2b. DECLASSIFICATION/DOWNGRADING SCHEDULE	Approved for public release; distribution unlimited

4. PERFORMING ORGANIZATION REPORT NUMBER(S)	5. MONITORING ORGANIZATION REPORT NUMBER(S)
TR-0090(5925-07)-1	SSD-TR-92-06

6a. NAME OF PERFORMING ORGANIZATION	6b. OFFICE SYMBOL (If applicable)	7a. NAME OF MONITORING ORGANIZATION
The Aerospace Corporation Technology Operations		Space Systems Division

6c. ADDRESS (City, State, and ZIP Code)	7b. ADDRESS (City, State, and ZIP Code)
El Segundo, CA 90245-4691	Los Angeles Air Force Base Los Angeles, CA 90009-2960

8a. NAME OF FUNDING/SPONSORING ORGANIZATION	8b. OFFICE SYMBOL (If applicable)	9. PROCUREMENT INSTRUMENT IDENTIFICATION NUMBER
		F4701-88-C-0089

8c. ADDRESS (City, State, and ZIP Code)	10. SOURCE OF FUNDING NUMBERS			
	PROGRAM ELEMENT NO.	PROJECT NO.	TASK NO.	WORK UNIT ACCESSION NO.

11. TITLE (Include Security Classification)

Total-Dose-Induced Charge Buildup in Nitrided-Oxide MOS Devices

12. PERSONAL AUTHOR(S)

Krantz, Richard J. and Scarpulla, John

13a. TYPE OF REPORT	13b. TIME COVERED FROM _____ TO _____	14. DATE OF REPORT (Year, Month, Day) 1992 April 23	15. PAGE COUNT 25

16. SUPPLEMENTARY NOTATION

17. COSATI CODES			18. SUBJECT TERMS (Continue on reverse if necessary and identify by block number)
FIELD	GROUP	SUB-GROUP	Electron Trapping
			Nitridation
			Simulation

19. ABSTRACT (Continue on reverse if necessary and identify by block number)

Nitrided oxides and reoxidized, nitrided oxides processed at various nitridation temperatures for various nitridation times have been irradiated. The total-dose response of these nitrided oxides has been analyzed and compared to that of radiation-hard control oxides. To aid in the analysis, the charge trapping model of Krantz et al. [1987] has been extended to include electron trapping and qualitatively applied to simulate the experimental results. Nitridation temperature was found to have a significant effect on the radiation response of thin (~ 150 Å) nitrided oxides and reoxidized, nitrided oxides. The data show that oxides nitrided at 1050°C and reoxidized accumulate less fixed charge (by a factor of ~ 2) than the control oxides. Oxides nitrided at 950°C and reoxidized accumulate substantially more fixed charge (by a factor of ~ 5) than the controls or any of the nitrided samples. The analysis indicates that nitridation creates neutral hole traps as well as neutral electron traps, and that reoxidation can decrease the concentration of both hole and electron traps.

20. DISTRIBUTION/AVAILABILITY OF ABSTRACT	21. ABSTRACT SECURITY CLASSIFICATION
[X] UNCLASSIFIED/UNLIMITED [ ] SAME AS RPT. [ ] DTIC USERS	Unclassified

22a. NAME OF RESPONSIBLE INDIVIDUAL	22b. TELEPHONE (Include Area Code)	22c. OFFICE SYMBOL

DD FORM 1473, 84 MAR   83 APR edition may be used until exhausted. All other editions are obsolete.

CONTENTS

FIGURES

I. INTRODUCTION

Interest in nitrided silicon dioxide as the gate dielectric in MOS structures has increased because this material promises greater reliability in stressing environments [1–4]. Recently, the radiation hardness of reoxidized nitrided oxides has been shown to be superior to that of thin oxides [5–7]. In this report we present the results of total-dose testing of thin nitrided oxides that have been nitridized at temperatures of 950, 1050, 1100, and 1150°C for nitridation times of 45 to 300 sec. The radiation response of these nitrided oxides is compared to that of an unnitridized, radiation hard, control oxide. Various nitridized oxides were reoxidized for 30 sec at 1150°C and total-dose irradiated. These results are compared to those of the nonirradiated control and nitrided oxides.

To aid in the analysis of these results, the radiation-induced charge-trapping model of Krantz et al. [8] has been extended to include electron trapping and applied to the experimental data to simulate the results. Parameters derived from the simulation are used to interpret qualitatively trends in the data in terms of electron and hole trap distributions.

The data will show that oxides nitridized at 950°C, whether reoxidized or not, accumulated substantially more fixed charge than either the control oxides or any of the other nitridized oxides. Samples nitrided at 1100 or 1150°C, reoxidized or not, will be shown to exhibit a radiation response similar to that of the control oxides. On average, the reoxidation of oxides nitrided at 1050°C will be shown to accumulate less fixed charge than did the controls.

The analysis will indicate that (1) the nitridation of oxides creates hole traps as well as electron traps, (2) the location of hole and electron traps depends on nitridation time, and (3) the concentration (and location) of hole and electron traps depends on whether or not nitridized oxides are reoxidized.

In Section II the experimental details and the measurement results are given and discussed. In Section III a summary of the trapping model of Krantz et al. [8], relevant to the experimental conditions, is given, the model is extended to include electron trapping, and the details of the data simulation are described. In Section IV the experimental results are discussed in light of the model and simulation results. We conclude by summarizing our findings in Section V.

Accession For

NTIS GRA&I ☑
DTIC TAB ☐
Unannounced ☐
Justification_____

By_____
Distribution/

Availability Codes

| Dist | Avail and/or Special |

A-1

3

II. EXPERIMENTAL DETAILS/RESULTS

Capacitors were fabricated using a low temperature, radiation-hardened gate oxide process. The starting substrates were n-type, 0.6 ohm-cm (1×10^{16} cm^{-3} doping density) material. The oxide thickness was 150 Å. The oxides were nitrided for times from 45 to 300 sec at temperatures ranging between 950 and 1150°C. For reoxidized samples, reoxidation was done from 1000°C to 1150°C and for times from 30 to 120 sec. The gate electrodes were formed from 3000-Å POCl3-doped polysilicon with an evaporated 3000-Å Ti layer and a 3000-Å Al layer. The capacitors were defined by means of a dry-etch lithographic step.

Pre- and post-irradiation midgap voltages were determined from high-frequency (1 MHz) C–V measurements. Irradiations were performed in a 10–keV x-ray test system at a dose rate of 250 krad(Si)/min. Capacitors were biased at –5, 0, and +5 V during irradiations. The C–V measurements were performed in situ. The maximum dose delivered was 5 Mrad(Si). Shown in Figures 1 through 5 is the radiation response versus total dose of various samples. The response is shown as the midgap voltage shift normalized by q t_{ox}/ϵ, where q is the elemental charge, t_{ox} is the dielectric (oxide, nitrided oxide, or reoxidized nitrided oxide) thickness and ϵ is the permittivity of the dielectric. The response is given in units of 1×10^{10} cm^{-2} and denoted as "Effective Fixed Charge Density." This normalization was chosen to normalize the effects of slightly different permittivities of the nitrided oxide films and the slightly increased dielectric thickness of the reoxidized films. For example, the largest dielectric constant measured for the nitrided oxides was about 4.15 and the reoxidized film thicknesses were nominally about 161 Å. All other samples, oxide and nitrided oxide, were 150 Å thick.

In all figures the open circles represent the zero-gate-bias results, the plus signs represent the positive-bias (+5 V) results, and the crosses represent the negative-bias (–5 V) results. To guide the eye, the solid curves, which are exponential fits to the data of the form $N_0[1 - \exp(-D/D_0)]$, where D is the total dose, are shown. For convenience, the conversion from effective fixed-charge density to midgap voltage shift is given in each figure. The vertical axes in Figures 1 through 4 are close to 200 mV full scale when converted to midgap voltage shifts. The vertical axis in Figure 5 is about 100 mV full scale when converted.

Figure 1 shows the radiation response of the radiation-hard, unnitrided control oxide. The results shown in Figure 1 are as expected for the radiation response in oxides, i.e., the positive-bias results exceed those for negative bias, which in turn are larger than the zero-bias results. This is true over the whole range of total dose, from 0.0 to 5 Mrad(Si).

Figures 2 through 4 show the radiation responses of samples nitrided at 1150°C for 60, 150, and 300 sec, respectively. For the sample nitrided for 60 sec, the negative-bias results are worse over the whole total-dose range than either the positive- or zero-bias results.
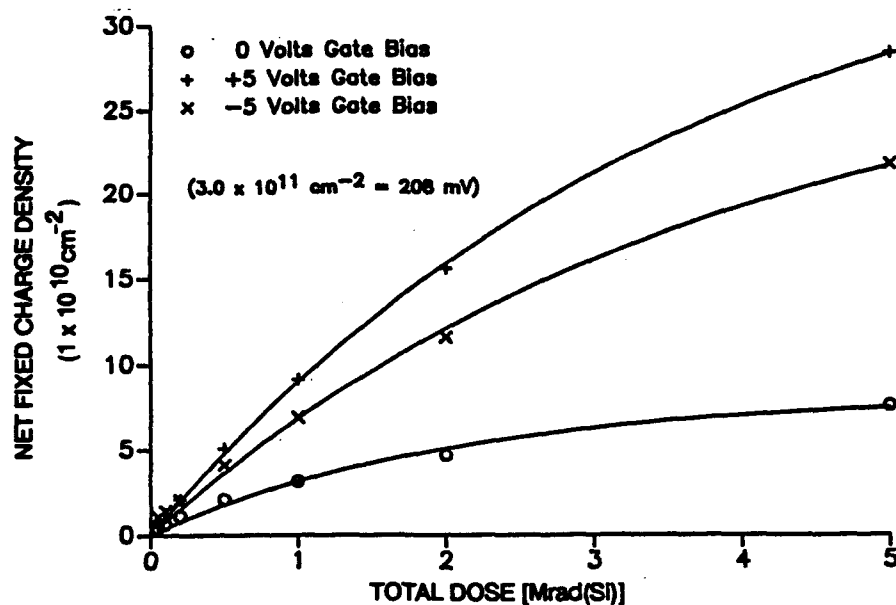
5

Figure 1. The effective fixed-charge density of the 150-Å rad-hard control oxide (in 1×10^{10} cm^{-2}) vs total dose for a +5-V gate bias (plus signs), a –5-V gate bias (crosses), and a 0.0-V gate bias (circles). Measured data are represented by the symbols. The curves are exponential fits (see text) to the data.

Figure 2. The effective fixed-charge density (in 1×10^{10} cm^{-2}) for oxides nitridized at 1150°C for 60 sec vs total dose for a +5-V gate bias (plus signs), a –5-V gate bias (crosses), and a 0.0-V gate bias (circles). Measured data are represented by the symbols. The curves are exponential fits (see text) to the data.

6
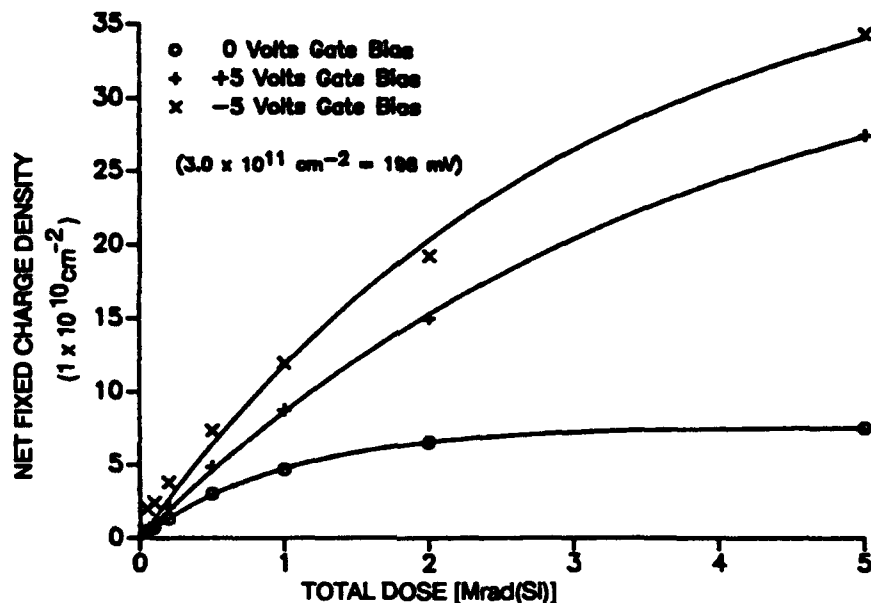
Figure 3. The effective fixed-charge density (in 1×10^{10} cm^{-2}) for oxides nitridized at 1150°C for 150 sec vs total dose for a +5-V gate bias (plus signs), a –5-V gate bias (crosses), and a 0.0-V gate bias (circles). Measured data are represented by the symbols. The curves are exponential fits (see text) to the data.
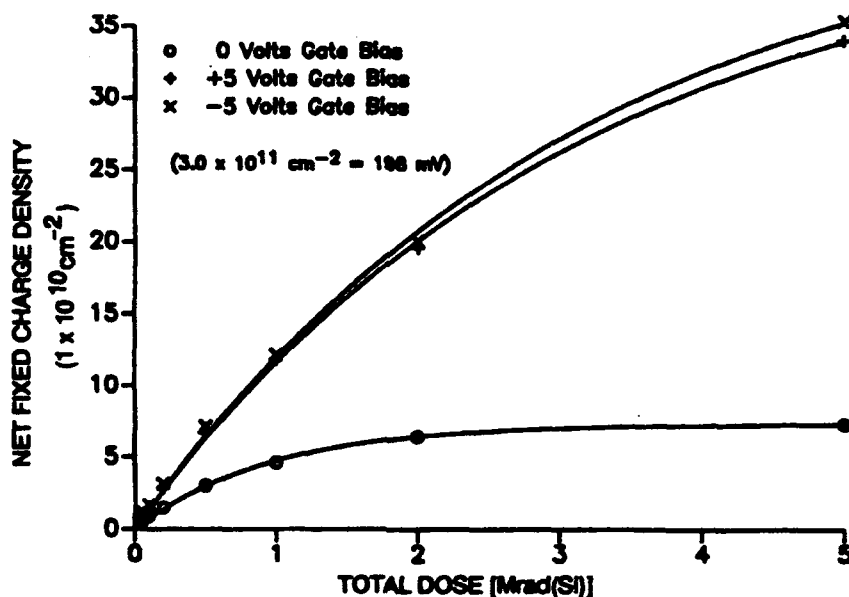
Figure 4. The effective fixed-charge density (in 1×10^{10} cm^{-2}) for oxides nitridized at 1150°C for 300 sec vs total dose for a +5-V gate bias (plus signs), a –5-V gate bias (crosses), and a 0.0-V gate bias (circles). Measured data are represented by the symbols. The curves are exponential fits (see text) to the data.
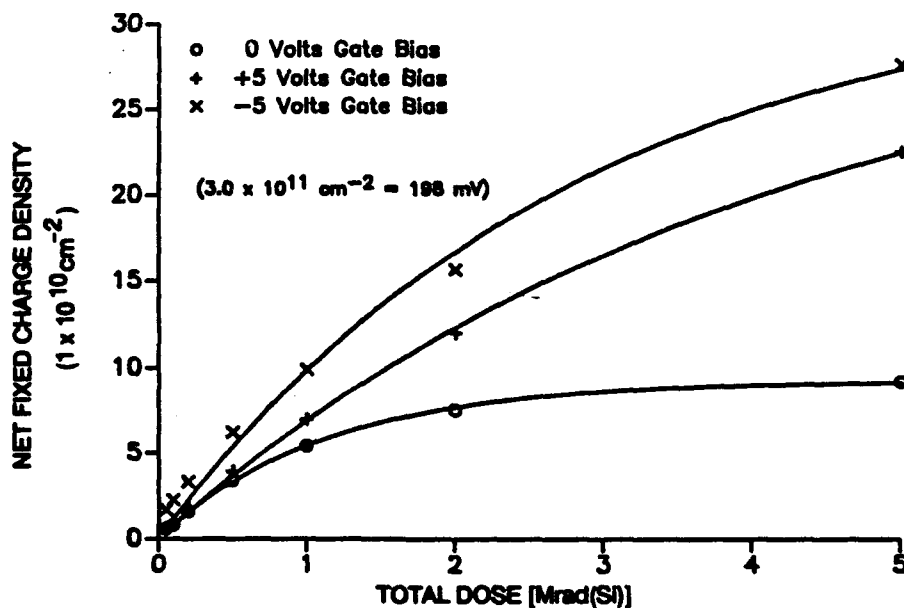
Figure 5. The effective fixed-charge density (in 1×10^{10} cm^{-2}) for a reoxidized nitrided oxide nitridized at 1050°C for 120 sec and reoxidized at 1150°C for 30 sec vs total dose for a +5-V gate bias (plus signs), a -5-V gate bias (crosses), and a 0.0-V gate bias (circles). Measured data are represented by the symbols. The curves are exponential fits (see text) to the data.
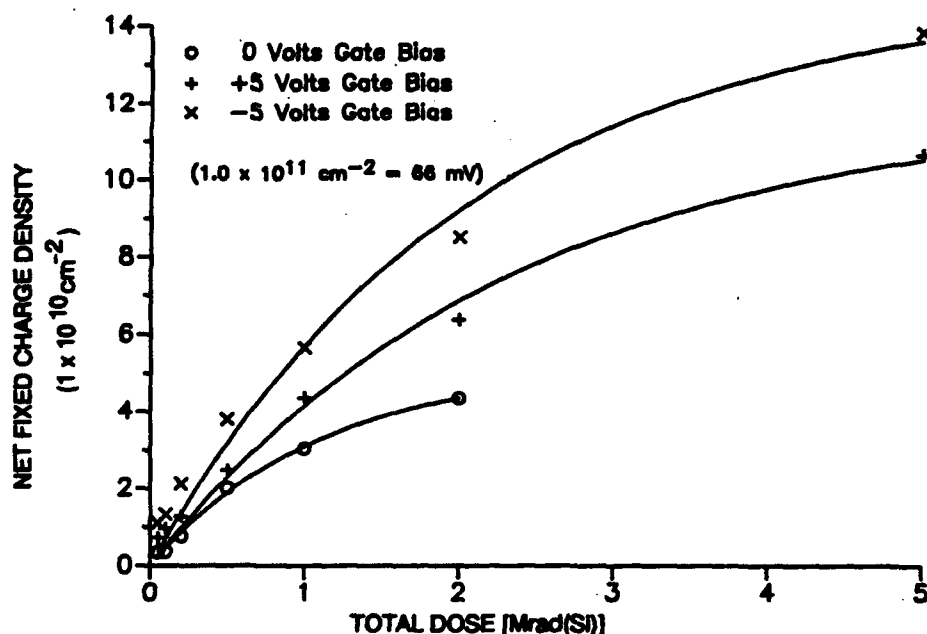
The magnitude of the negative-bias response in this sample is about the same as that of the positive-bias response in the control oxide shown in Figure 1. This behavior can be explained by the introduction of hole traps near the gate, as well as by the introduction of electron traps with nitridation. The increase in the zero-bias radiation response, compared to that of the control oxide, can also be explained by the introduction of hole traps during nitridation. Part of the increase in the zero-bias results of Figure 2 may be accounted for by a slightly increased average electric field across the sample (which decreases geminate recombination, yielding more carriers available for trapping). The larger field is due to a larger flat-band voltage (-0.46 V) in this sample as a result of nitridation.

Figure 3 shows the results for samples nitrided at 1150°C for 150 sec. Qualitatively these results are very similar to the results shown in Figure 2 (i.e., the negative-bias response exceeds the positive-bias response and at zero bias the response is less than either the positive- or the negative-bias results over the whole range of total dose). The major difference is that the positive- and negative-bias responses are larger by about 14% than the positive- and negative-bias responses of samples nitrided for 60 sec. This can be explained by a further simultaneous increase of hole and electron traps with nitridation. The zero-bias results are reduced relative to those shown in Figure 2 and may be explained by the introduction of electron traps.

8

Figure 4 shows the radiation response for samples nitrided at 1150°C for 300 sec. The positive- and negative-bias results are almost indistinguishable from the negative-bias result for the sample nitrided for 150 sec. This result is consistent with a simultaneous increase in the first moments of the neutral hole and electron trap distributions.

The radiation response of samples nitrided at 1050°C for 120 sec and reoxidized at 1100°C for 30 sec (see Figure 5) is much improved over that of the control oxide (97 mV full scale versus 208 mV full scale). This result can be explained by a decrease in the concentration of hole traps in the dielectric as a result of reoxidation. Note that the zero-bias radiation response is also reduced in these samples, which is consistent with this explanation.

Altogether, some 39 nitrided oxide samples, 15 of which were reoxidized, were irradiated along with 6 oxide control samples. The role of nitridation temperature is summarized in Figure 6, which shows the maximum radiation-induced effective fixed charge versus nitridation temperature for all samples. Note that the vertical scale is logarithmic. Nitrided oxides processed at 1050°C are better (have less effective fixed charge) on average than those processed at any of the other temperatures and are better on average than the control oxides for all biases.

Furthermore, the reoxidation of films nitrided at 1150°C showed only marginal improvement in radiation response compared to the nonreoxidized samples, and the reoxidation of oxides nitrided at 1100°C degrades the radiation response slightly. A very large degradation in radiation response is seen in reoxidized films that were nitrided at 950°C. Reoxidized films
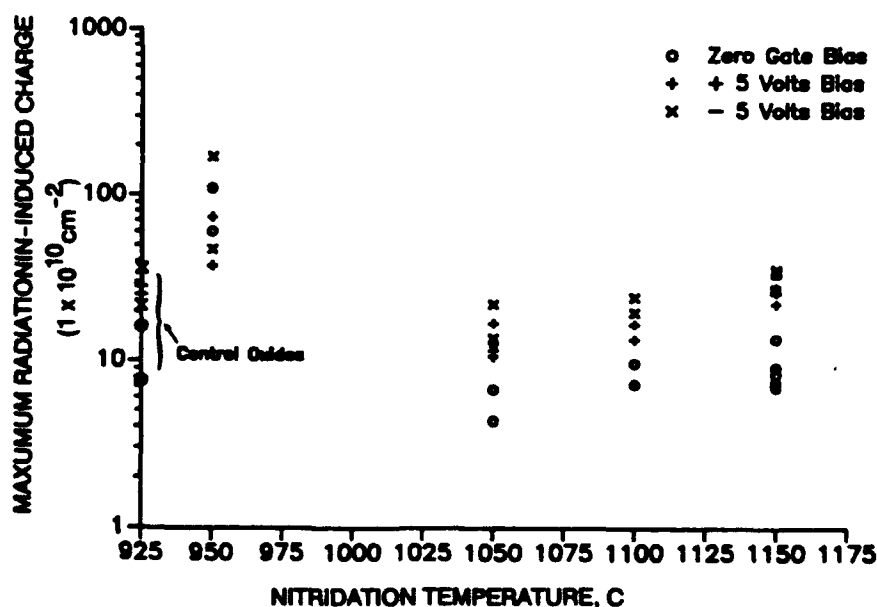
Figure 6. Maximum effective fixed charge (in 1×10^{10} cm^{-2}) vs nitridation time. The plus signs represent a +5-V gate bias during irradiation, crosses denote a –5-V gate bias, and circles denote zero gate bias.

nir.ided at 1050°C show a substantial decrease, by a factor of 2, in radiation response compared to the control samples and by far exhibit the best radiation response of the nitrided/re-oxidized samples.

In the next section, the charge trapping model of Krantz et al. [8] is summarized and extended to charge trapping in nitrided oxide films. To aid in the analysis of the measurements cited above, a simulation based on the extended theory is developed. In Section IV the simulation results are discussed.

III. THEORY EXTENSION/SIMULATION

A. THEORY SUMMARY

It is convenient to begin by considering the continuity equation for trapped holes:

$$dP_T(x,t)/dt = \sigma_d[E(x,t)] \, j_p(x,t) \, [P(x,t) - P_T(x,t)]$$

$$- \sigma_c[E(x,t)] \, j_n(x,t) \, P_T(x,t) \tag{1}$$

$$- g[x,E(x,t]] \, P_T(x,t)$$

where

$P_T(x,t)$ = the position (x)- and time (t)-dependent trapped-hole concentration,

$\sigma_d[E(x,t)]$ = the local electric-field [E(x,t)]-dependent neutral (dipole-induced) hole capture cross section,

$\sigma_c[E(x,t)]$ = the local electric-field-dependent coulombic electron capture cross section,

$j_p(x,t)$ = the radiation-induced hole flux,

$j_n(x,t)$ = the radiation-induced electron flux,

$P(x,t)$ = the neutral hole-trap concentration, and

$g[x,E(x,t)]$ = the WKB tunneling rate for holes.

(For a discussion of the details of the charge trapping model summarized here, refer to Krantz et al. [8].)

The first term in Eq. (1) describes hole trapping at unoccupied, neutral hole traps. The second term describes electron trapping at occupied hole traps (i.e., coulombic electron traps). The third term describes the tunneling of holes out of occupied hole traps.

The solution of Eq. (1) may be simplified by assuming: that (1) the electric-field dependence of the tunneling term may be ignored [8] (in the WKB approximation the tunneling rate is only weakly dependent on electric field), (2) the field dependence of the capture cross sections may be described by an average electric field [8], and (3) the neutral hole-trap concentration is time-independent.

To effect a closed-form solution of Eq. (1), the valence-band hole and conduction-band electron continuity equations must be considered. The valence-band hole continuity equation may be written, assuming a constant electric field in terms of the hole flux, thus:

$$v_p^{-1} dj_p(x,t)/dt = (D_h/v_p)\ d^2j_p(x,t)/dx^2$$

$$\pm\ dj_p/dx\ +\ n_0\ D\phi\ -\ \sigma_0 j_p(x,t) \tag{2}$$

$$[P(x,t) - P_T(x,t)]$$

where

v_p = the velocity of holes in the valence band,

D_h = the diffusion coefficient for valence-band holes,

n_0 = the radiation-induced hole-generation rate ($\sim 8 \times 10^{12}$ rad^{-1} cm^{-3}),

$\dot{D}$ = the dose rate in rads, and

ϕ = the fraction of carriers that escape recombination (yield).

(Note that the field dependence of the capture cross sections has been suppressed for convenience.)

The first term on the right-hand side of Eq. (2) is due to diffusion. The second term on the right-hand side is the field dominated term (the negative sign denotes a positive electric field and the positive sign denotes a negative electric field). The third term is the radiation-induced source term. The last term describes the loss of carriers as a result of trapping at unoccupied hole traps.

The measurements cited in the previous section were done under steady-state and high electric-field conditions. Irradiations were performed for tens of seconds or longer. As transit times for electrons and holes across oxides less than 1000 Å thick are on the order of fractions of picoseconds and fractions of microseconds, respectively, the steady-state assumption is reasonable.

At high electric fields the second term of Eq. (2) dominates the diffusion term throughout the bulk of the dielectric. For example, the diffusion term is comparable to the field term only within a distance much less than $(kT/q)/E$ from the boundaries, where the mobile-hole density approaches zero. At 0.1 MV/cm and room temperature, diffusion dominates at distances much less than 30 Å from the boundaries. Because tunneling of charge out of the dielectric depletes trapped charge tens of angstroms into the dielectric, the details of the valence-band hole distribution in this region may be ignored for fields of the order of 0.1 MV/cm.

For example, for the positive-bias measurements (strong accumulation) a +5-V bias dropped across a 150-Å dielectric layer yields an average field of +3.33 V/cm. Negative bias (strong inversion; after a 0.7-V drop across the silicon depletion layer is accounted for, yields an average field of -2.88 MV/cm. Even at zero gate bias, a typical flat-band voltage of -0.18 V yields an average field of +0.12 MV/cm across the dielectric. Therefore, the diffusion term in Eq. (2) may be ignored.

Equation (2) may be simplified further by considering that the magnitude of the trapping term, the last term on the right-hand side of this equation, is a maximum when $j_p(x)$ is equal to $N_0 D\phi t_{ox}$ and $P_T(x)$ is equal to zero. The maximum possible error introduced by neglecting the trapping of valence-band holes (large carrier sweep-out) is equal to $P(x) \sigma_d t_{ox}$ and occurs only near the boundaries.

The capture cross section, σ_d, is on the order of 10^{-10} cm^2 (or less) and t_{ox} is about 150 Å. $P(x)$ may be estimated from the data cited in the previous section. The measured effective fixed-charge densities at large doses saturate at values typically near 3.0×10^{11} cm^{-2}, which yields an average concentration for a 150-Å film of 2.0×10^{17} cm^{-3}. If we assume that at saturation most of the neutral hole traps are filled, 2.0×10^{17} cm^{-3} is a reasonable estimate of $P(x)$. With these values the maximum possible error introduced by ignoring the trapping term is 3.0×10^{-3}. Therefore, the trapping term can be neglected.

Under these conditions, Eq. (2) can be solved to yield

$$j_p(x) = j_0 \pm n_0 D\phi x \tag{3}$$

where j_0 depends on the boundary conditions. For positive gate bias (plus sign) the hole flux is assumed to be zero at the gate ($x = 0.0$) and j_0 is zero. For negative gate bias (minus sign) the hole flux is assumed to be zero at the dielectric/silicon interface ($x = t_{ox}$) and j_0 is equal to $n_0 D\phi t_{ox}$.

The continuity equation for the conduction-band electrons may be similarly solved to yield the electron flux for positive *and* negative electric fields, respectively:

$$j_{n+}(x) = n_0 D\phi(t_{ox} - x) \tag{4a}$$

$$j_{n-}(x) = n_0 D\phi x \tag{4b}$$

The substitution of Eqs. (3) and (4) into Eq. (2) allows for a solution, assuming there is a constant dose rate D and no trapped holes are present at $t = 0.0$. The solution, after some manipulation, for the dose-dependent trapped-hole distribution under positive bias is given by

$$P_T + (x,D) = W_p + (x) P(x)\{1 - \exp[-D/D_p + (x)]\} \tag{5a}$$

where

$$W_{p+}(x) = \sigma_d j_{p+}(x) / [\sigma_d j_{p+}(x) + \sigma_c j_{p+}(x) + g(x,E)] \tag{5b}$$

and

$$+ D_{p+}(x) = D / [\sigma_d j_{p+}(x) + \sigma_c j_{n+}(x) + g(x,E)] \tag{5c}$$

and the quantity Dt has been replaced by the total dose D. A similar expression results for the negative-bias case.

The effective fixed charge, as defined in the previous section, is the first moment of the charge distribution averaged over the thickness of the dielectric layer. Under positive bias, the effective fixed charge is

$$P_{eff+}(D) = (1/t_{ox}) \int x \, P_{T+}(x,D)dx \qquad (6)$$

A similar expression results for the case of negative bias.

B. THEORY EXTENSION

We assume that electron traps, presumably at nitrogen sites in nitrided oxides, can be described as neutral (dipole-induced) traps, that trapped electrons act as coulombic hole traps, and that the tunneling of electrons out of the dielectric can be described by a WKB tunneling rate. Therefore, the trapped-electron continuity equation is analogous to Eq. (1) for trapped holes.

The continuity equations for valence-band holes and conduction-band electrons are similar to Eq. (2). Under steady-state and high electric fields (including the large sweep-out of carriers), Eqs. (3) and (4), for the radiation-induced hole and electron fluxes, are valid. The solution of the trapped-electron continuity equation for a constant dose rate, no radiation-induced trapped electrons at t = 0.0, and positive bias yields

$$N_{T+}(x,D) = W_{n+}(x) \, N(x)\{1 - \exp[-D/D_{n+}(x)]\} \qquad (7a)$$

where

$$W_{n+}(x) = \sigma_d \, j_{n+}(x)/[\sigma_d \, j_{n+}(x) + \sigma_c \, j_{p+}(x) + g(x,E)] \qquad (7b)$$

and

$$D_{n+}(x) = D/[\sigma_d \, j_{n+}(x) + \sigma_c \, j_{p+}(x) \qquad (7c)$$

where, for convenience, the tunneling rate for electrons out of the dielectric is assumed to be equal to the tunneling rate for holes. In this case N(x) is the neutral electron trap concentration. All other quantities are defined as before. A similar expression is obtained for negative bias. This leads to an expression similar to Eq. (6) for the effective electron fixed charge (positive bias):

$$N_{eff+}(D) = (1/t_{ox}) \int (x) \, N_{T+} (x,D) \, dx \qquad (8)$$

A similar expression results for the case of negative bias.

When both neutral hole and electron traps are present, as is postulated for nitrided oxides, the net effective fixed charge (for positive bias), P_{net+}, is the difference between Eqs. (6) and (8). Thus,

$$P_{net+}(D) = P_{eff+}(D) - N_{eff+}(D) \tag{9}$$

For negative bias a similar result is obtained. Experimentally, if midgap voltage shifts are negative, as is the case for the data cited in the previous section, then $P_{net\pm}(D)$ is positive and hole trapping is dominant.

C. DATA SIMULATION

Although it has been shown that neutral hole traps are due to oxygen vacancies and that electron trapping probably occurs at nitrogen sites in nitrided oxides, the details of the neutral hole-trap and neutral electron-trap distributions are unknown. Therefore, we have assumed that these distributions can be simulated by separate delta-function distributions of the form

$$P(x) = N_{HO} \cdot \delta(x - X_{HO}) \tag{10a}$$

and

$$N(x) = N_{EO} \cdot \delta(x - X_{EO}) \tag{10b}$$

where N_{HO} is the magnitude (in cm^{-2}) of the delta-function neutral hole-trap distribution and X_{HO} is the location in the dielectric of this distribution. Similarly, N_{EO} and X_{EO} are the magnitude and location, respectively, of the delta-function neutral electron-trap distribution.

Although this is a rather severe assumption, without knowledge of the neutral hole-trap or electron-trap distributions we are forced to use stylized trap distributions to simulate the data. We have tried, with little success, to simulate these data with constant neutral trap distributions. This approach fails because the assumption of a constant distribution fixes the position of the first moment of the distribution at the midpoint of the dielectric. This turns out to be more restrictive than assuming a delta-function distribution that allows for both the magnitude and the position of the distribution to be used to fit the data.

It will be shown below that the delta-function distributions simulate the data reasonably well and that the comparison of the fitting parameters defined in Eqs. (10a) and (10b) can be used to describe qualitatively the changes in the neutral trap distributions with processing (i.e., with nitridation and reoxidation).

Substituting Eqs. (10a) and (10b) into Eqs. (5a) and (7a), effecting the integrations in Eqs. (6) and (8), and evaluating Eq. (9) yields the simulation results for the effective fixed charge (positive bias):

$$P_{sim+}(D) = N_{HO} W_{p+}(X_{HO})\{1 - \exp[-D/D_{p+}(X_{HO})]\} - N_{EO} W_{n+}(X_{EO})$$
$$\{1 - \exp[-D/D_{n+}(X_{EO})]\} \tag{11}$$

where $W_{p+}(x)$, $W_{n+}(x)$, $D_{p+}(x)$, and $D_{n+}(x)$ are defined as before. A similar expression is obtained for the negative-bias case.

The total dose dependence exhibited in Eq. (11) is more complicated than the $N_o[1 - \exp(-D/D_o)]$ form shown in Figures 1 through 4. The data shown in those figures suggest a more complicated form, particularly for negative bias, as the data consistently show a somewhat "stretched-out" total-dose response compared to the simple curve fits. The form of Eq. (11) (and the negative-bias equivalent) allows for this more complicated dependence.

In the next section the qualitative features of these simulations will be compared and discussed in light of the data shown in Figures 1 through 6. All values of the model parameters are equivalent to those used previously by Krantz et al. [8]. The field dependence of the capture cross sections has been incorporated and the average electric field internal to the dielectric has been corrected for the presence of trapped charge.

IV. DISCUSSION

Figures 7 through 11 show the simulations for the control oxide of Figure 1 and the nitrided oxides of Figures 2 through 5.

Figure 7 shows the simulation for the control sample. No electron trapping is included in this simulation (i.e., $NE_0 = 0.0$). The positive-bias response is larger than the negative-bias response over the whole range of total dose. This corresponds to the data shown in Figure 1. A slightly different dose dependence is seen for the positive and negative biases (i.e., the negative-bias response saturates at a slightly lower dose). This difference is due to the effect of the field on the capture cross sections. At $+5$ V the field across the oxide is 3.33 MV/cm, whereas at -5 V the field is -2.88 MV/cm, as a result of a voltage drop of about 0.7 V in the silicon depletion layer. At these fields the coulombic electron-capture cross sections are relatively constant. The neutral dipole hole-capture cross sections are several percent smaller at the larger field. This causes the positive-bias response to saturate at a slightly lower dose than the negative-bias response.

The zero-bias results are lower than either the positive-bias or negative-bias results, as a result of geminate recombination. The relatively small electric field in the dielectric at zero bias, about $+0.12$ MV/cm, separates only some 30% of the radiation-generated charge. The rest of the charges recombine before separation and trapping can occur.

In Figure 8 the simulation for the oxide nitridized at 1150°C for 60 sec is shown. The parameters used to simulate these data are shown in the figure. The position of the neutral hole-trap distribution, X_{HO}, has been held constant. The addition of electron trapping causes the negative-bias radiation response to exceed the positive-bias results. To simulate these responses, a neutral electron-trap delta-function distribution near the gate is necessary. Under positive bias, substantial electron trapping occurs near the gate, a result of the relatively large concentration of electrons available for trapping. Under negative bias, little electron trapping occurs because the concentration of electrons in the conduction band available for trapping is small at X_{EO}. Therefore, the negative-bias radiation response is larger because there is not enough electron trapping to mitigate the effects of hole trapping. The zero-bias response is still dominated by geminate recombination.

For the magnitudes of the simulated results shown in Figure 8 to correspond roughly to the data shown in Figure 2, a hole-trap concentration of 3.44×10^{12} cm^{-2} was assumed. The neutral hole-trap concentration is larger than that used for the control oxide simulation shown in Figure 7. It may be inferred from this result that nitridation creates not only electron traps but also hole traps as well.

Figures 9 and 10 show simulations for samples nitrided at 1150°C for 150 and 300 sec, respectively. In the case of the simulation of the data for the samples nitrided for 150 sec, the concentration of both the neutral electron and neutral hole traps must be increased for the
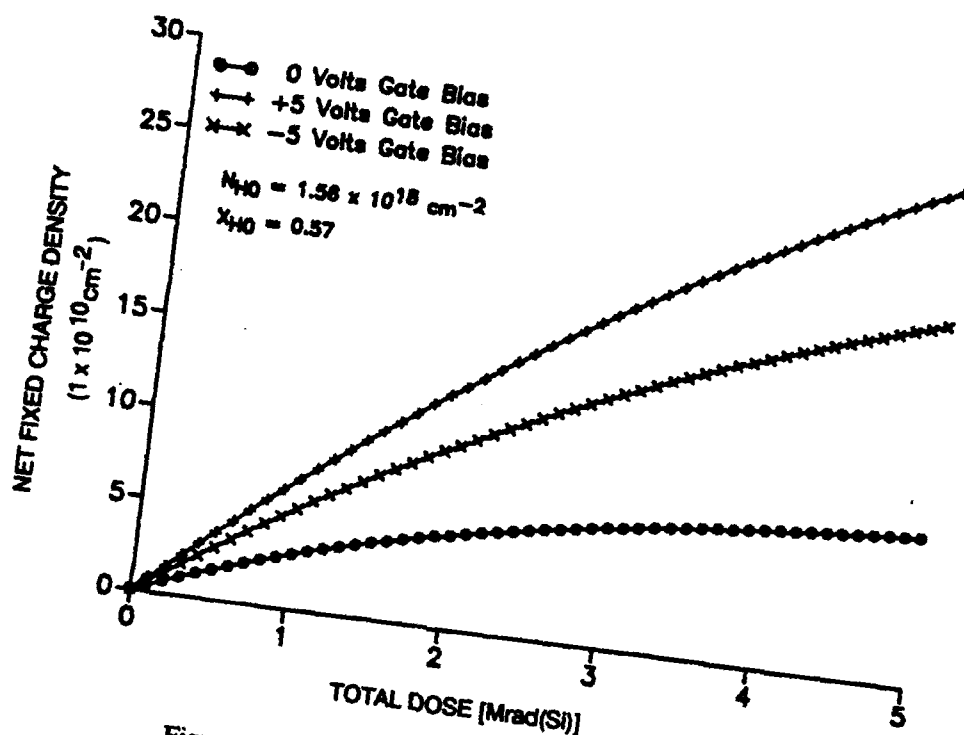
17

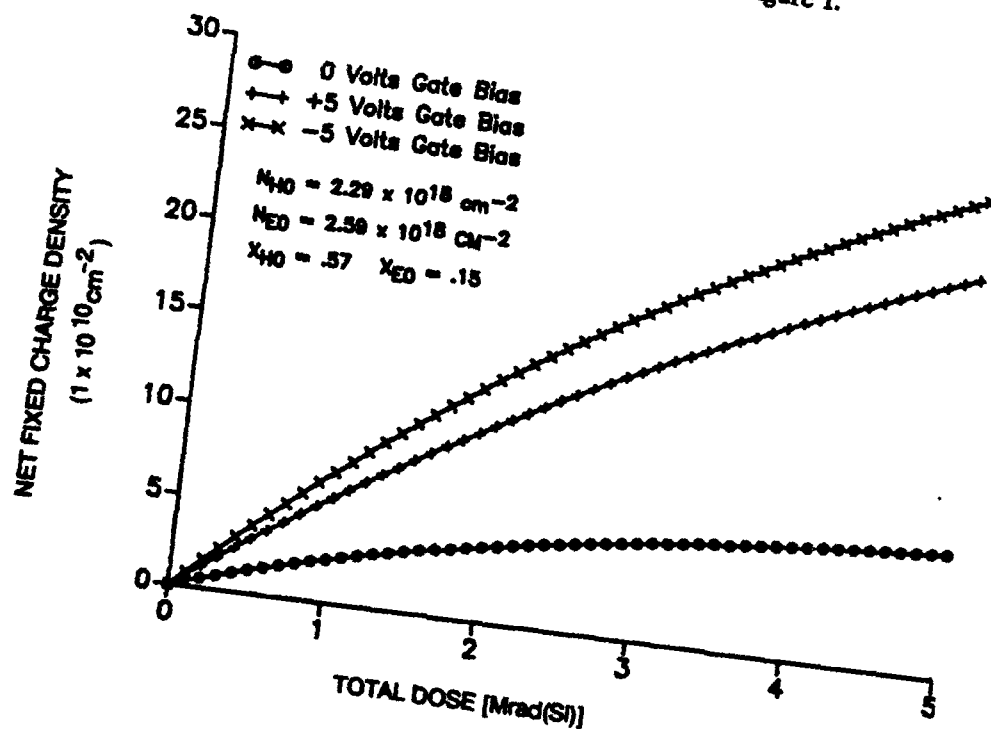Figure 7. Simulation of the data shown in Figure 1.

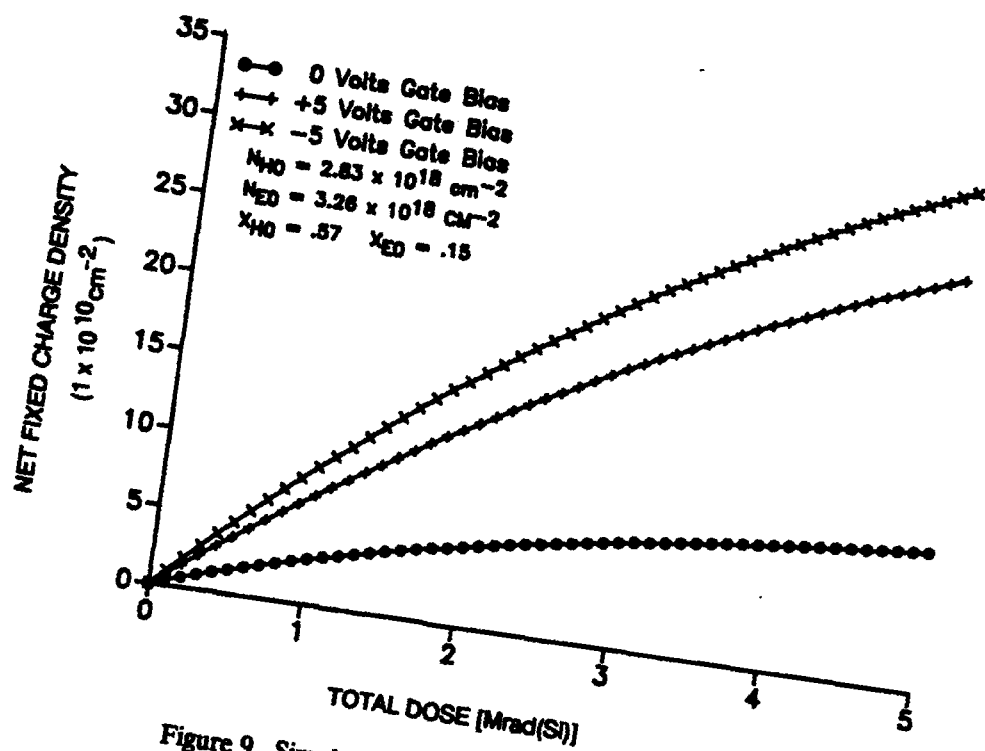Figure 8. Simulation of the data shown in Figure 2.

18

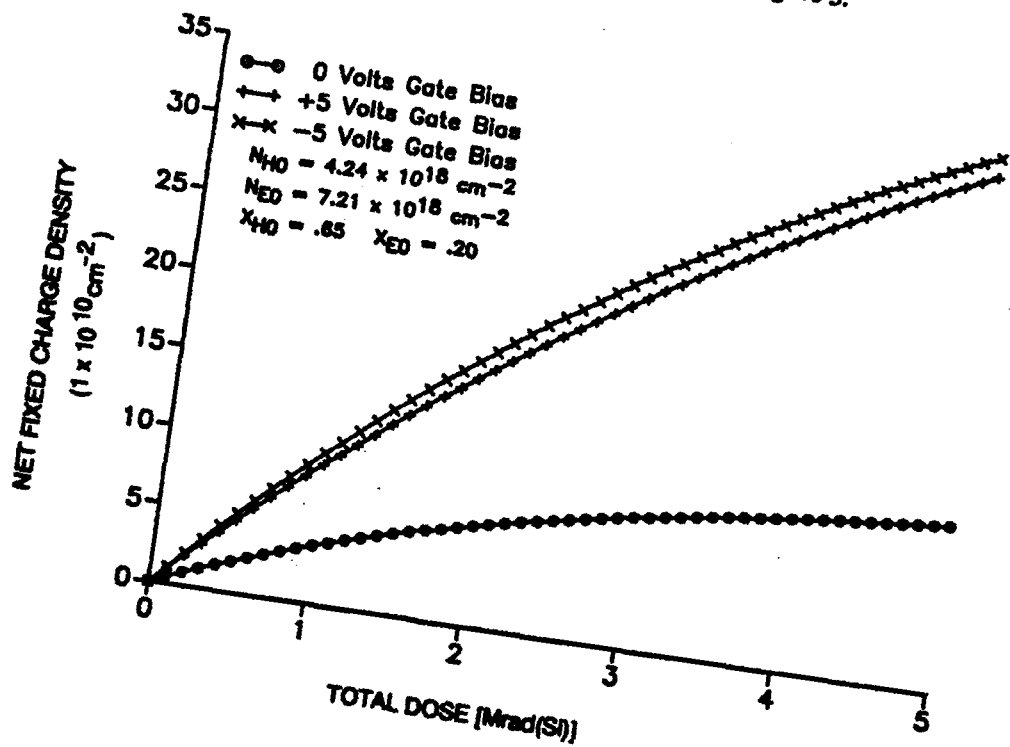Figure 9. Simulation of the data shown in Figure 3.

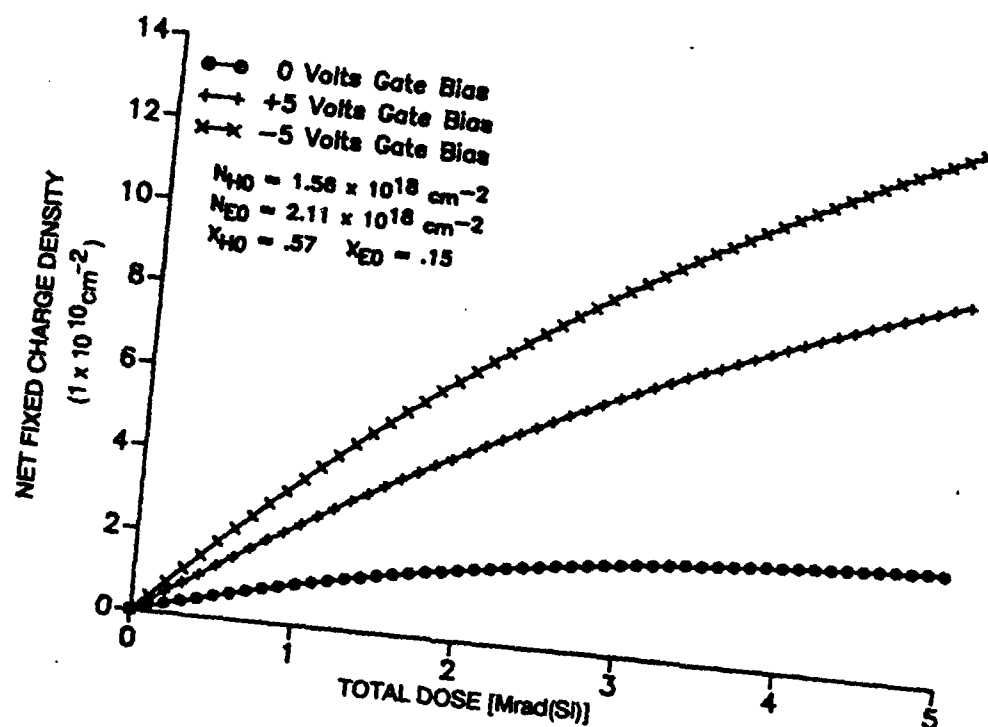Figure 10. Simulation of the data shown in Figure 4.

19

Figure 11. Simulation of the data shown in Figure 5.

simulation to correspond to the data. This lends support to the idea that nitridation creates hole traps as well as electron traps.

The simulation shown in Figure 10, for samples nitrided at 1150°C for 300 sec, shows that not only are the concentrations of neutral electron and hole traps increased but also that the distributions are concentrated deeper in the dielectric, i.e., closer to the dielectric/silicon interface. This is consistent with the idea that longer nitridation times not only create more traps but also drive the traps closer to the dielectric interface.

Shown in Figure 11 are the simulations for the radiation response of the reoxidized samples shown in Figure 5. The parameters shown in the figure indicate that a much lower neutral hole-trap concentration is necessary to represent the data. The 5-Mrad(Si) points are reasonably represented, but the low-dose region is much "flatter" than the data indicate. This failure of the simulation at low doses for these results is due, in part, to the fact that, because of increased processing, the neutral hole-trap and neutral electron-trap distributions are much more extended in the dielectric than is the case for the oxides or nitrided oxides. In this case, representing the distributions as delta-functions is a gross simplification.

The simulation results are summarized in Table I.

As shown in Table I, as samples were nitrided for longer and longer times (60 to 300 sec) the simulation results indicate that more and more neutral hole and electron traps are created (i.e., both N_{HO} and N_{EO} increased with nitridation time compared to the control sample).

20

Also, the position of both distributions moves deeper into the dielectric with nitridation time (i.e., X_{HO} and X_{EO} increase with nitridation time).

Shown in the third column of Table 1 are the products of the magnitude and position of the neutral hole–trap and neutral electron-trap distributions. This quantity corresponds to the average first moment of the delta-function distribution. As expected from the results in columns 1 and 2, this quantity, for both hole and electron traps, increases with nitridation time also. The last row of Table I shows the simulation results for a reoxidized, nitrided oxide sample. Both the neutral hole-trap and neutral electron-trap concentrations are reduced relative to any of the nitrided samples, and the values of X_{HO} and X_{EO} are the same as the values for the samples nitrided for 60 and 150 sec.

Although only a semiquantitative correspondence is possible between the simulated results and the data, we can explain the qualitative aspects of the experimental results in terms of only N_{HO}, N_{EO}, X_{HO}, and X_{EO}. For a meaningful quantitative comparison to be made between the theory and the experimental results, the details of the neutral hole-trap and neutral electron-trap distributions must be known.

Table 1. Summarization of Simulation Results

Samples	N_{HO} (N_{EO}) cm^{-2}	X_{HO}/t_{ox} (X_{EO}/t_{ox})	$N_{HO}X_{HO}/t_{ox}$ ($N_{EO}X_{EO}/t_{ox}$) cm^{-2}
Control	2.35×10^{12}	0.57	1.33×10^{12}
	(0.0)	——	(0.0)
Nitrided (RTN 1150°C)			
60 sec	3.44×10^{12}	0.57	1.96×10^{12}
	(3.89×10^{12})	0.15	(5.84×10^{11})
150 sec	4.25×10^{12}	0.57	4.42×10^{12}
	(4.89×10^{12})	(0.15)	(7.33×10^{11})
300 sec	6.36×10^{12}	0.65	4.13×10^{12}
	(1.08×10^{13})	(0.20)	(2.16×10^{12})
Reoxidized (RTN 1050°C Reox 120 sec)	2.34×10^{12} (3.17×10^{12})	0.57 (0.15)	1.33×10^{12} (4.76×10^{11})

V. SUMMARY

We have reported the results of total-dose testing of thin nitrided oxides that have been nitridized at temperatures of 950, 1050, 1100, and 1150°C for nitridation times of 45 to 300 sec. The radiation response of these nitrided oxides was compared to that of an unnitridized, radiation hard, control oxide. Various nitridized oxides were reoxidized for 30 sec at 1150°C and total-dose irradiated. These results were compared to those of the nonirradiated control and nitrided oxides.

The data show that nitrided oxides nitridized at 950°C, whether reoxidized or not, accumulated substantially more fixed charge than either the control oxides or any of the other nitridized oxides. Samples nitrided at 1100 or 1150°C, reoxidized or not, exhibited a radiation response similar to that of the control oxides. On average, the reoxidation of oxides nitrided at 1050°C accumulated less fixed charge than did the controls.

To aid in the analysis of these results, the radiation-induced charge-trapping model of Krantz et al. [8] was extended to include electron trapping and applied to the experimental data, using delta-function neutral trap distributions, to simulate the results. Parameters derived from the simulation were used to interpret, qualitatively, trends in the data in terms of electron-trap and hole-trap distributions.

The simulation results indicate that (1) the nitridation of oxides creates hole traps as well as electron traps, (2) the location of hole and electron traps depends on nitridation time, and (3) the concentration (and location) of hole and electron traps depends on whether or not nitridized oxides are reoxidized.

REFERENCES

1. G. J. Dunn, "Hole Trapping in Reoxidized Nitrided Silicon Dioxide," *J. Appl. Phys.* **65** (12), 4879 (15 June 1989).

2. M. M. Moslehi et al., "Rapid Thermal Nitridation of SiO$_2$ for Nitroxide Thin Dielectrics," *Appl. Phys. Lett.* **47** (10), 1113 (15 November 1985).

3. J. Nulman and J. P. Krusius, "Rapid Thermal Nitridation of Thin Thermal Silicon Dioxide Films," *Appl. Phys. Lett.* **47** (2), 148 (15 July 1985).

4. M. L. Naiman et al., "The Constitution of Nitrided Oxides and Reoxidized Nitrided Oxides on Silicon," *J. Appl. Phys.* **58** (2), 779 (15 July 1985).

5. R. Sundaresan, et al., "Rapid-Thermal Nitridation of SiO$_2$ for Radiation-Hardened MOS Gate Dielectrics," *IEEE Trans. Nuc. Sci.* NS–33 (6), 1223 (December 1986).

6. R. K. Pancholy and F. M. Erdman, "Radiation Effects on Oxynitride Gate Dielectrics," *IEEE Trans. Nuc. Sci.* NS–30 (6), 4141 (December 1983).

7. G. J. Dunn and P. W. Wyatt, "Reoxidized Nitrided Oxide for Radiation-Hardened MOS Devices," *IEEE Trans. Nuc. Sci.* NS–36 (6), 2161 (December 1989).

8. R. J. Krantz, L. W. Aukerman, and T. C. Zietlow, "Applied Field and Total Dose Dependence of Trapped Charge Buildup in MOS Devices," *IEEE Trans. Nuc. Sci.* NS–34 (6), 1196 (December 1987).

TECHNOLOGY OPERATIONS

The Aerospace Corporation functions as an "architect-engineer" for national security programs, specializing in advanced military space systems. The Corporation's Technology Operations supports the effective and timely development and operation of national security systems through scientific research and the application of advanced technology. Vital to the success of the Corporation is the technical staff's wide-ranging expertise and its ability to stay abreast of new technological developments and program support issues associated with rapidly evolving space systems. Contributing capabilities are provided by these individual Technology Centers:

Electronics Technology Center: Microelectronics, solid-state device physics, VLSI reliability, compound semiconductors, radiation hardening, data storage technologies, infrared detector devices and testing; electro-optics, quantum electronics, solid-state lasers, optical propagation and communications; cw and pulsed chemical laser development, optical resonators, beam control, atmospheric propagation, and laser effects and countermeasures; atomic frequency standards, applied laser spectroscopy, laser chemistry, laser optoelectronics, phase conjugation and coherent imaging, solar cell physics, battery electrochemistry, battery testing and evaluation.

Mechanics and Materials Technology Center: Evaluation and characterization of new materials: metals, alloys, ceramics, polymers and their composites, and new forms of carbon; development and analysis of thin films and deposition techniques; nondestructive evaluation, component failure analysis and reliability; fracture mechanics and stress corrosion; development and evaluation of hardened components; analysis and evaluation of materials at cryogenic and elevated temperatures; launch vehicle and reentry fluid mechanics, heat transfer and flight dynamics; chemical and electric propulsion; spacecraft structural mechanics, spacecraft survivability and vulnerability assessment; contamination, thermal and structural control; high temperature thermomechanics, gas kinetics and radiation; lubrication and surface phenomena.

Space and Environment Technology Center: Magnetospheric, auroral and cosmic ray physics, wave-particle interactions, magnetospheric plasma waves; atmospheric and ionospheric physics, density and composition of the upper atmosphere, remote sensing using atmospheric radiation; solar physics, infrared astronomy, infrared signature analysis; effects of solar activity, magnetic storms and nuclear explosions on the earth's atmosphere, ionosphere and magnetosphere; effects of electromagnetic and particulate radiations on space systems; space instrumentation; propellant chemistry, chemical dynamics, environmental chemistry, trace detection; atmospheric chemical reactions, atmospheric optics, light scattering, state-specific chemical reactions and radiative signatures of missile plumes, and sensor out-of-field-of-view rejection.